

Original paper

Obsidian balls (marekanite) from Cerro Tijerina, central Nicaragua: petrographic investigations

Štěpánka MRÁZOVÁ^{1*}, Petr GADAS²¹ Czech Geological Survey, Klárov 3, 118 21 Prague 1, Czech Republic; stepanka.mrazova@geology.cz² Joint Laboratory of Electron Microscopy and Microanalysis, Department of Geological Sciences, Masaryk University, Kotlářská 2, 611 37 Brno, Czech Republic

* Corresponding author



The paper describes a find of volcanic glass in central Nicaragua. We investigated obsidian samples in perlite from a large profile of volcanic rocks (Cerro Tijerina) in the vicinity of the town of Matagalpa. The obsidian occurs in the form of up to 3-cm dark-coloured balls (spheres) randomly distributed in brittle grey perlite, which also has spherulitic texture. These balls, previously called marekanite, are characterised by an abundance of microphenocrysts (feldspar, biotite, amphibole, apatite and magnetite). Microprobe analysis of the homogenous glass of obsidian balls and perlite has confirmed their subalkaline, and particularly high-K calc-alkaline character ($\text{SiO}_2 \geq 70\%$, $\text{Na}_2\text{O} + \text{K}_2\text{O} < \text{Al}_2\text{O}_3$), which is typical of rhyolitic melts. A sharp contact was observed between the core and the surface layer (approx. 0.1–0.2 mm) of the obsidian balls, reflecting changes in the H_2O content.

Keywords: obsidian, marekanite, volcanic glass, Cerro Tijerina, Nicaragua

Received: 9 November 2010; **accepted:** 21 March 2011; **handling editor:** R. Skála

1. Introduction

Obsidian is a volcanic acidic glassy rock associated with perlite. The latter is a grey bulky volcanic rock of similar chemical composition, but with fluidal texture and numerous concentric cracks resembling fragments of pearls. The obsidian balls (spheres) occurring in perlite, usually smaller than 5 cm in diameter and having an indented surface, are called marekanite. They received their name after the place where they were first discovered, Marekanka near Okhotsk in Siberia, Russia (Judd 1886). Another term for spherically shaped obsidians, used especially by mineral collectors and gemmologists, is “Apache tears”. The obsidian balls, differing from the surrounding perlite by a lower water content (Johannsen 1932; Ljunggren 1960), are coloured in various shades, most commonly from smoke-grey to black.

Perlite is formed from volcanic glasses of dacitic and rhyolitic composition by hydration and alteration, i.e., by a change in the mineralogy and texture due to the action of hot or cold aqueous solutions or gases. These processes are caused by meteoric water rather than by the water-rich original magma (Friedman and Smith 1958; Friedman et al. 1966). However, a controversy exists concerning the parameters of perlite formation (diffusion coefficient of water, activation energy of hydration) (Friedman et al. 1966; Marshall 1961). The degree of perlitization also depends on the total volatile contents and temperature (Denton et al. 2009). The alteration of

perlitized obsidian was shown to result in the dissolution of glass and crystallization of secondary minerals (smectite, zeolite), as well as in a change in the colour from dark grey to green or dull brown (Noh and Boles 1989; Denton et al. 2009).

The objective of this paper is to describe the petrographic characteristics of the obsidian balls found, for the first time, in the volcanic area of Nicaragua. The finding of obsidian in Nicaragua so far consisted in block-shaped material or Indian tools made of obsidian brought from other regions of Central America.

2. Geological setting

The investigated area is located in central Nicaragua, which is built mainly by Palaeogene calc-alkaline volcanic rocks – lavas and extensive acid–intermediate ignimbrites. The main volcanic phase took place in Oligocene, when numerous rhyolite calderas were formed.

The Cerro Liquidambar volcanic group, named after its dominant peak (1375 m a.s.l.) (N 12°58′17.48″; W 85°59′24.99″), was investigated in detail as a part of a regional study carried out by the Czech Geological Survey (Hradecký et al. 2002). It is located NW of the town of Matagalpa (Fig. 1). The Cerro Tijerina ridge (1375 m a.s.l.) is a dominant feature of the volcanic group.

The rock types and their succession were characterized in a profile (Fig. 2) on the south-eastern slopes of the Cerro Tijerina Massif – Cerro El Ocote, rising from

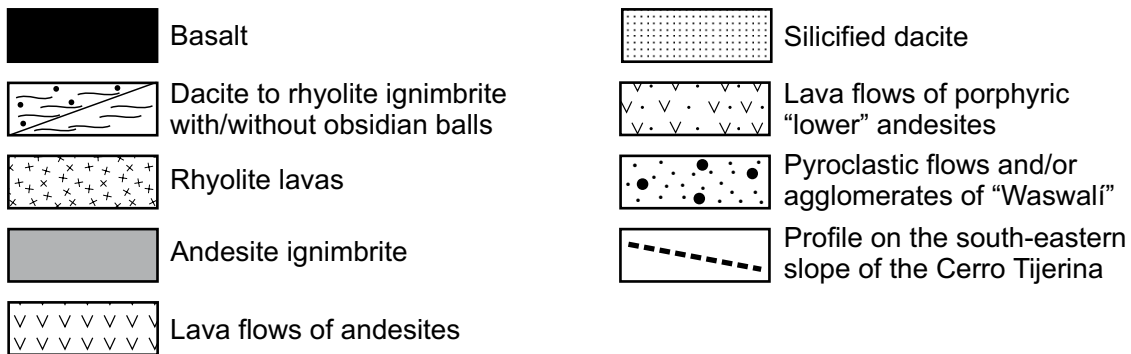
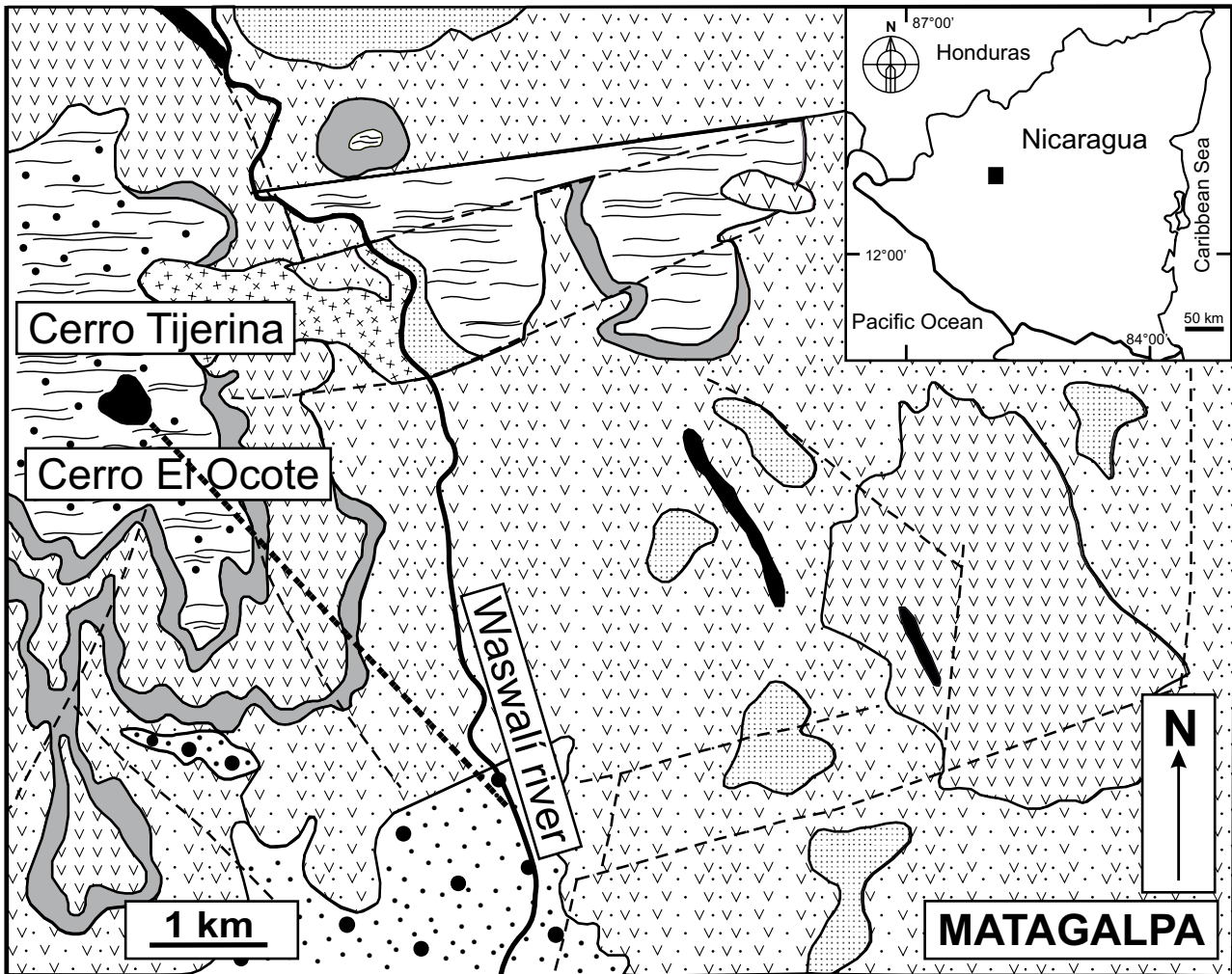


Fig. 1 Geological sketch map of the Cerro Liquidámbar volcanic group.

the Waswali river valley up to the summit. In total, seven layers were distinguished.

1. The base of the profile is formed by coarse-grained pyroclastic flows and/or agglomerates of the so-called "Waswali" type. The pyroclastic flows are typically of yellow-green colour and consist of layers containing angular and subangular fragments of altered andesites

with a size up to 0.4 m, often cross-cut by fine-grained basaltic dykes.

2. The "Waswali" volcanoclastics are extensively covered by layers of medium-grained porphyric lower andesites, with tabular or spheroidal jointing and lateritic weathering on their top, with a total thickness of up to 220 m.

3. A layer of fine-grained andesitic ignimbrites with a fluidal texture, up to 20 m thick, was found on the southern slope of Cerro El Ocote, whereas towards the north they wedge out or terminate on tectonic dislocations.

4. The andesite ignimbrites are covered by younger, andesite to basaltic andesite lava flows that pass upwards to autoclastic breccia. These lava flows are up to 30 m in thickness. The autoclastic breccia is porphyric, fine to medium grained, formed by clasts of variable sizes with vesicular or compact texture. It has very frequently undergone lateritic weathering. The compact lava flows that typically display tabular jointing are covered by a massive complex of ignimbrites.

5. The lower ignimbrite layer, up to 30 m in thickness, is formed by a red-coloured andesite ignimbrite which is fine-grained to compact, very often silicified, with well-developed fluidal texture, containing elongate microcrystalline aggregates of quartz and cristobalite. The upper part of the red andesite ignimbrite is locally rheomorphically deformed with the next ignimbrite layer, which probably has dacitic composition and is strongly silicified. Both rocks form an extensively rheomorphically folded complex up to 40 m in thickness. No andesite ignimbrites were found above this andesite–dacite complex.

6. The uppermost part of the massive ignimbrite complex is built by silicified, dacite to rhyolite ignimbrites and rhyolite lavas up to 220 m in thickness. This layer is formed by fine-grained to breccia-type ignimbrites with grey perlite formations of spherulitic texture, containing balls (up to 2 cm in diameter) of black obsidian – marekanite (Fig. 3), chalcedony, devitrified glass and scarce microphenocrysts (feldspar, biotite, amphibole, apatite, magnetite).

7. The top of Cerro Tijerina is formed by the relict of lava flows of strongly altered, vesicular basalt.

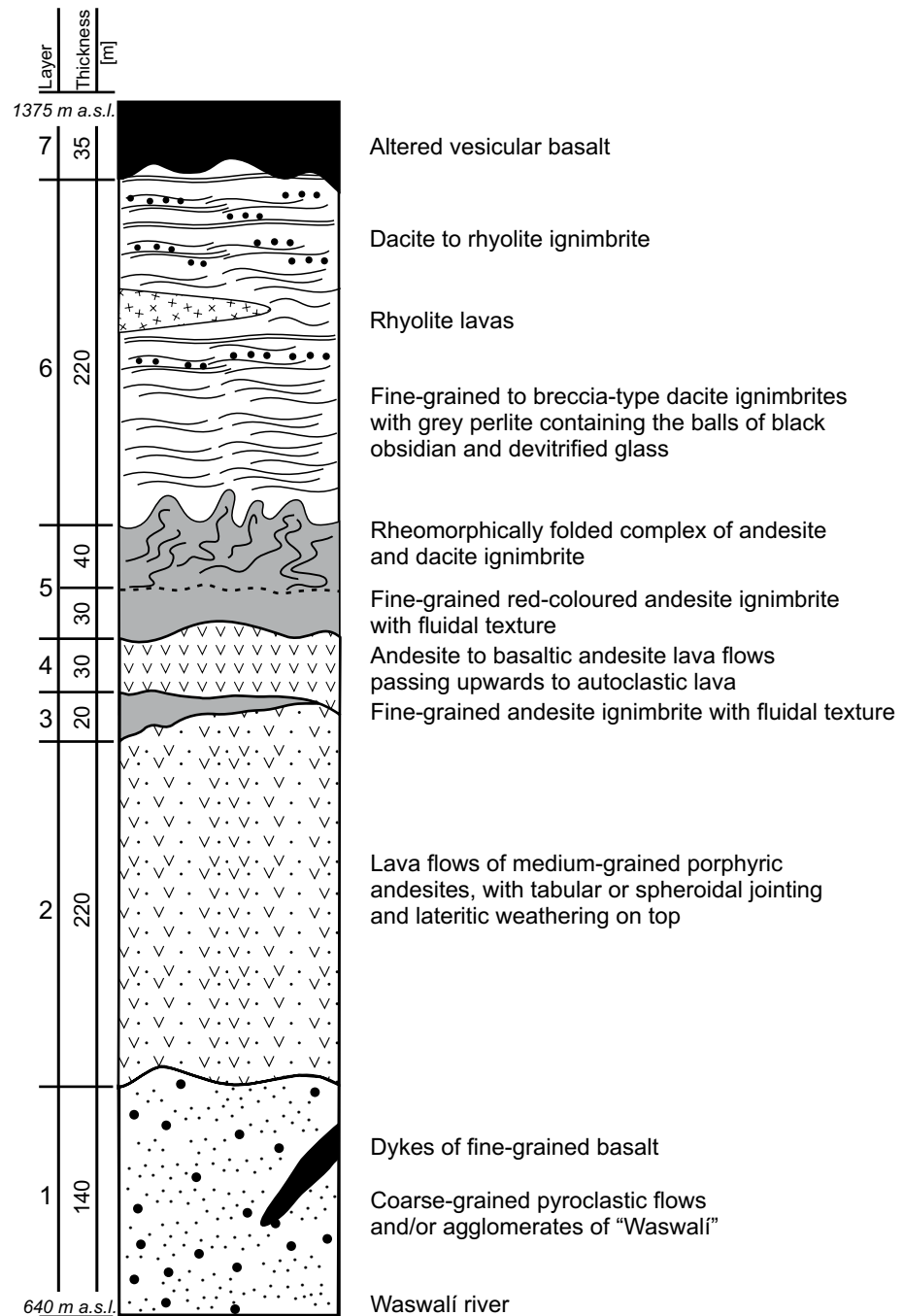


Fig. 2 Simplified profile on the eastern slopes of the Cerro Tijerina – Cerro El Ocote Massif.

The geological structure of other parts of the Cerro Liquidámbar volcanic group differs somewhat from that of Cerro Tijerina. The common feature of the group consists in the presence of lower andesite lavas with andesite to dacite ignimbrites. However, no analogue of the unique profile of Cerro Tijerina with its sequence of volcanic rock types and occurrence of black obsidian balls was found in other parts of Cerro Liquidámbar.

3. Methods



Fig. 3 Photograph of obsidian balls (marekanite).

The chemical analyses of minerals were performed on a CAMECA SX100 electron microprobe at the Joint Laboratory of Electron Microscopy and Microanalysis, Department of Geological Sciences, Masaryk University and the Czech Geological Survey in Brno equipped with a wavelength dispersive spectrometer. The following conditions were used: accelerating voltage of 15 kV, probe current of 10 nA and defocused beam of 5 μm diameter. The range of counting times was 10–20 s for major elements and 20–40 s for minor and trace elements. The following standards and analytical (K_{α}) lines were used: almandine (Fe²⁺, Si), wollastonite (Si), grossular (Al, Ca), MgO (Mg), sanidine (K), titanite (Ti), spessartine (Mn), NaCl (Cl), fluorapatite (Ca, P), topaz (F), baryte (Ba); (L_{α}) lines: CePO₄ (Ce), LaPO₄ (La) and (L_{β}) lines: benit-

Tab. 1 Electron-microprobe data of glass from obsidian balls and perlite (wt. %)

Sample No.	SM1-1C	SM1-1C	SM1-1C	SM1-1C	SM1-1C	SM1-1C	SM1-1C	SM1-1C	SM1-2C	SM1-2C	SM1-2C	SM1-2C	SM1-2C
Analysis No.	1	2	3	4	5	6	7	8	9	10	11	12	12
SiO ₂	76.316	77.166	77.303	75.409	76.415	76.533	77.305	76.526	76.701	76.630	77.613	77.201	77.201
TiO ₂	0.160	0.155	0.134	0.189	0.140	0.160	0.156	0.148	0.141	0.164	0.174	0.127	0.127
Al ₂ O ₃	13.034	12.598	12.909	12.472	12.894	12.848	12.898	12.881	12.892	13.023	12.984	12.993	12.993
FeO	0.582	0.376	0.747	0.677	0.767	0.825	0.862	0.704	0.776	0.697	0.253	0.499	0.499
MnO	0.063	b.d.1	b.d.1	b.d.1	b.d.1	b.d.1	b.d.1	b.d.1	b.d.1	0.114	0.095	b.d.1	b.d.1
MgO	0.150	0.120	0.131	0.139	0.149	0.167	0.194	0.183	0.150	0.159	0.045	0.095	0.095
CaO	0.793	0.807	0.781	0.865	0.797	0.798	0.865	0.831	0.837	0.825	0.782	0.721	0.721
Na ₂ O	3.142	3.315	3.040	2.599	3.510	2.943	3.428	3.539	3.333	3.291	3.250	3.140	3.140
K ₂ O	4.357	4.476	4.349	4.294	4.343	4.365	4.347	4.444	4.366	4.487	4.470	4.378	4.378
BaO	0.082	b.d.1	0.135	0.158	0.077	0.11	0.083	0.163	0.148	0.159	0.105	0.158	0.158
P ₂ O ₅	b.d.1	0.042	b.d.1	b.d.1	0.027	b.d.1	b.d.1	b.d.1	0.035	0.023	b.d.1	b.d.1	b.d.1
Cl	0.087	0.058	0.059	0.092	0.081	0.089	0.074	0.106	0.080	0.086	0.070	0.069	0.069
F	0.086	0.106	0.053	0.022	b.d.1	0.035	0.043	0.057	0.076	b.d.1	b.d.1	b.d.1	b.d.1
Total	98.884	99.289	99.689	96.991	99.302	98.986	100.277	99.646	99.598	99.692	99.903	99.447	99.447

Sample No.	SM1-2C	SM1-2C	SM1-1C	SM2-C	SM2-C	SM2-C	SM2-C	SM2-C	SM2-C	SM2-C	SM2-C	SM2-C	SM2-C
Analysis No.	13	14	15	16	17	18	19	20	21	22	23	24	24
SiO ₂	74.989	76.198	75.061	74.858	74.681	75.202	73.787	74.176	76.801	78.494	78.945	74.860	74.860
TiO ₂	0.160	0.144	0.157	0.137	0.134	0.142	0.134	0.132	b.d.1	b.d.1	b.d.1	b.d.1	b.d.1
Al ₂ O ₃	12.324	12.746	12.537	12.378	12.410	12.462	12.185	12.352	12.625	12.213	12.474	13.200	13.200
FeO	0.806	0.667	0.633	0.610	0.626	0.698	0.671	0.564	0.193	0.085	0.194	0.150	0.150
MnO	0.071	0.062	b.d.1	0.088	b.d.1	b.d.1	b.d.1	b.d.1	b.d.1	b.d.1	b.d.1	b.d.1	b.d.1
MgO	0.137	0.152	0.103	0.170	0.138	0.150	0.129	0.136	b.d.1	b.d.1	b.d.1	b.d.1	b.d.1
CaO	0.791	0.755	0.731	0.824	0.845	0.801	0.792	0.783	0.428	0.228	1.877	0.282	0.282
Na ₂ O	2.916	3.142	3.080	2.719	2.297	2.474	1.310	2.280	3.544	2.849	4.894	3.175	3.175
K ₂ O	4.166	4.301	4.334	4.218	4.895	4.183	4.892	4.757	4.859	5.967	0.749	6.374	6.374
BaO	0.109	0.082	0.076	0.048	0.224	0.126	0.085	0.111	0.942	0.372	0.165	1.180	1.180
P ₂ O ₅	0.053	b.d.1	b.d.1	b.d.1	b.d.1	b.d.1	b.d.1	0.029	b.d.1	0.027	b.d.1	b.d.1	b.d.1
Cl	0.071	0.079	0.117	0.071	0.067	0.065	0.085	0.086	b.d.1	b.d.1	b.d.1	b.d.1	b.d.1
F	b.d.1	b.d.1	b.d.1	b.d.1	b.d.1	b.d.1	b.d.1	b.d.1	b.d.1	b.d.1	b.d.1	b.d.1	b.d.1
Total	96.619	98.377	96.937	96.196	96.448	96.407	94.219	95.498	99.482	100.373	99.433	99.313	99.313

b.d.1. = below detection limit (all Cr₂O₃ values were below detection limit)

Note: Analyses 1–12 – non-hydrated glass from obsidian balls; analyses 13–15 – hydrated rim of obsidian balls; analyses 16–20 – perlite glass; analyses 21–24 – spherulite glass

oite (Ba) and NdPO_4 (Nd). The average detection limits and standard deviations (in parentheses) under these conditions were: ~ 1800 ppm (0.16) for Nd; ~ 1200 ppm (0.13) for Ba, La and F; 740 ppm (0.07) for Ce; ~ 700 ppm (0.64) for Ca; ~ 700 ppm (0.12) for Na; ~ 670 ppm (0.06) for Mn; ~ 500 – 600 ppm (0.04–0.08) for S and Fe; ~ 400 ppm (0.4) for P and ~ 200 – 300 ppm (0.02–0.04) for Si, Al, Mg, K and Cl. The raw data were reduced using PAP matrix corrections (Pouchou and Pichoir 1985). The apatite mineral formula was calculated on basis of 26 anions and a sum of (F, Cl, OH) = 2.

4. Petrography

Obsidian balls reaching up to 2 cm in size (Fig. 3) show macroscopically sharp contact with the surrounding perlitite. They are black, non-transparent to semitransparent. When examined by electron microprobe (Tab. 1) the glass appears to be homogeneous except an up to 200 μm thick surface layer in contact with the perlitite (Fig. 4a). This layer exhibits slightly lower analytical totals of oxides (~ 97 – 98 wt. %), which is probably due to the elevated content of water. This area also bears signs of corrosion and concentric cracks in places. The surrounding perlitite has invariably lower sum of oxides (~ 96 – 96.5 wt. %) and exhibits compositional homogeneity under BSE. In contrast to the obsidian balls, the perlitite contains a large volume (estimated to 10–15 vol. %) of elongated bubbles, pores up to 0.5 mm in size, and rare spherulites composed of anhydrous and heterogeneous glass (Fig. 4c). Both the obsidian balls and perlitite contain numerous microphenocrysts that differ in quantity and composition. In the perlitite, the magnetite, which is up to 10 μm in size, is limonitized and subhedral; it occurs with rare anhedral apatite (< 20 μm), euhedral tabular feldspars (< 10 μm) and euhedral columnar amphiboles (< 10 μm). Subhedral magnetite up to 10 μm across can be observed in the obsidian balls (Fig. 4b), together with other microphenocrysts that are dispersed very irregularly in the glass. Amphibole microphenocrysts often show subparallel arrangement, thus enhancing the flow texture of the glass (Fig. 4b). Because of the insufficient size of the magnetite, feldspar and amphibole microphenocrysts, only apatite (Fig. 4a) was analysed quantitatively by the electron microprobe (Tab. 2). However, the ED spectra indicated that magnetite has a significant content of Ti, feldspar seems to be an oligoclase with significantly increased K and the composition of the amphiboles is close to magnesiohornblende.

Rare anhedral apatites up to 20 μm across usually occur in the outer parts of the obsidian balls. They are homogenous and exhibit slightly elevated contents of S (up to 0.048 apfu; 0.30 wt. % SO_2), Mn (up to 0.045 apfu

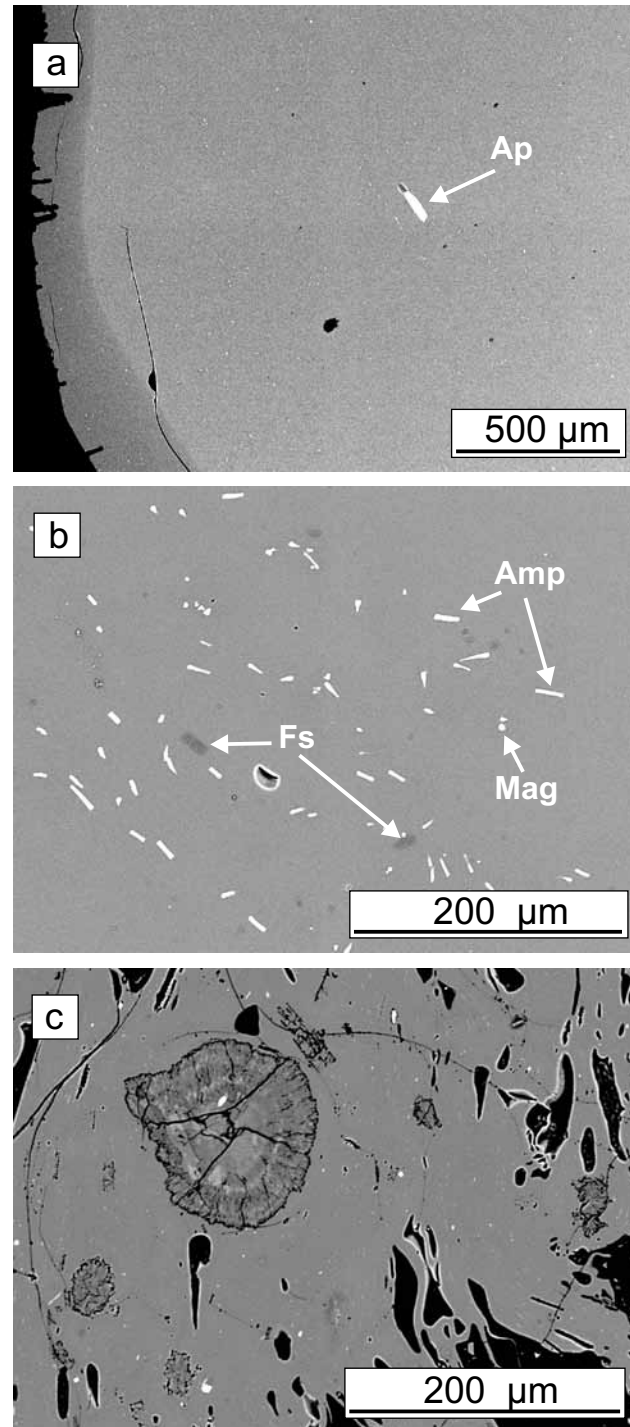


Fig. 4 Obsidian balls and perlitite, BSE images. **a** – Outer part of an obsidian ball with a microphenocryst of apatite; the hydrated, corroded, radially cracked concentric outer shell is darker in colour; **b** – Columnar microphenocrysts of feldspar, amphibole and magnetite; **c** – Perlitite glass rich in bubbles and containing conspicuous spherulites.

and 0.31 wt. % MnO), Mg (0.038 apfu and 0.15 wt. % MgO), Fe^{2+} (up to 0.068 apfu; 0.48 wt. % FeO) and REE (up to 0.030 apfu; 0.49 wt. % of REE oxides). As the fluorine predominates in the W site (0.950–1.071 apfu),

Tab. 2 Electron-microprobe data and empirical formulae of apatite microphenocrysts from obsidian balls

Sample No.	SM1-1C	SM1-2C	SM1-2C
Analysis No.	1	2	3
P ₂ O ₅	40.31	41.11	41.61
SiO ₂	0.34	0.17	0.25
SO ₂	0.30	0.25	0.18
La ₂ O ₃	0.10	0.10	b.d.l.
Ce ₂ O ₃	0.20	0.19	0.28
Nd ₂ O ₃	b.d.l.	0.20	0.20
CaO	55.52	55.57	55.18
FeO	0.48	0.23	0.23
MgO	0.15	0.15	0.15
MnO	0.31	0.28	0.25
Na ₂ O	0.24	0.16	0.09
K ₂ O	0.07	b.d.l.	0.06
F	1.96	2.01	1.79
Cl	1.49	1.43	1.38
H ₂ O*	0.46	0.46	0.59
O=Cl	-0.34	-0.32	-0.31
O=F	-0.83	-0.85	-0.75
Total	100.77	101.14	101.17
Calculated on basis of 26 anions and $\sum (F,Cl,OH) = 2$			
P	5.789	5.862	5.909
Si	0.058	0.029	0.042
S	0.048	0.039	0.028
Ca	10.091	10.028	9.917
Fe ²⁺	0.068	0.032	0.032
Mg	0.038	0.038	0.038
Mn	0.045	0.040	0.036
La	0.006	0.006	b.d.l.
Ce	0.012	0.012	0.017
Nd	b.d.l.	0.012	0.012
Na	0.079	0.052	0.029
K	0.015	b.d.l.	0.013
F	1.052	1.071	0.950
OH	0.520	0.521	0.658
Cl	0.428	0.408	0.392

* calculated value; b.d.l. = below detection limit

all the apatites correspond to apatite-(F), although they also show significantly elevated Cl (0.392–0.428 apfu).

The TAS classification diagram (Le Bas et al. 1986) (Fig. 5a) shows that both obsidian and perlite glasses belong to subalkaline series and correspond to rhyolite. However, the content of alkalis in the perlite is far more variable than in the obsidian. The classification diagram according to Peccerillo and Taylor (1976) (Fig. 5b) shows that both glasses are of high-K calc-alkaline composition.

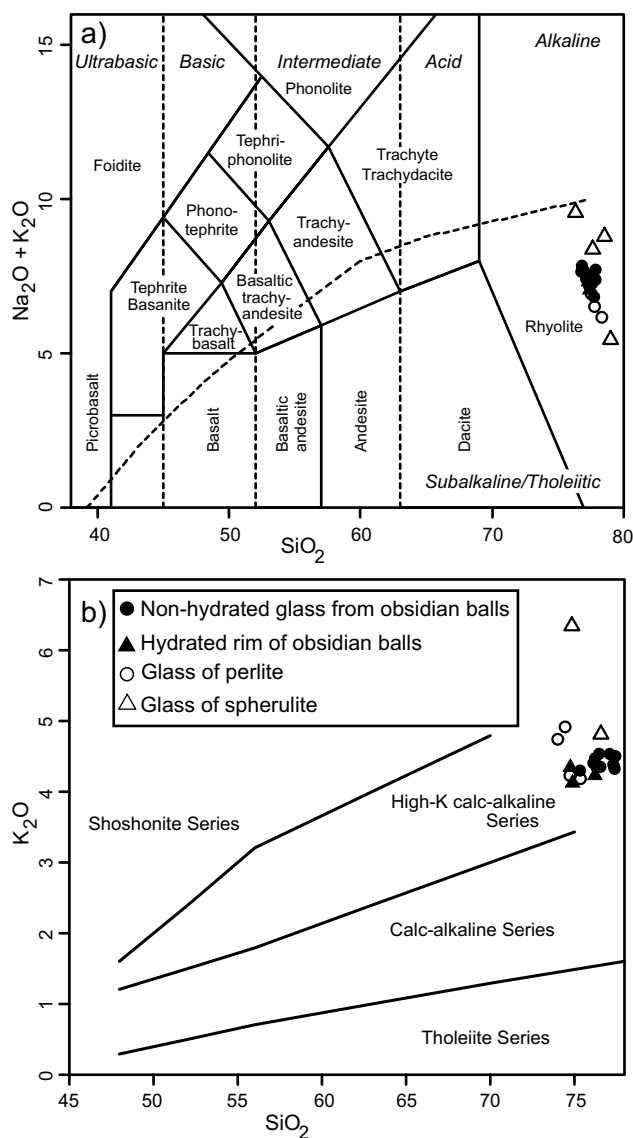


Fig. 5 Classification diagrams Na₂O + K₂O versus SiO₂ (Le Bas et al. 1986) (a) and K₂O versus SiO₂ (Peccerillo and Taylor 1976) (b) showing that the glass compositions are rhyolitic and high calc-alkaline (full symbols – obsidian, empty symbols – perlite).

5. Discussion and conclusions

The results reported in this paper provide evidence that the grey perlite with vesicular texture and the black obsidian glassy balls had a common evolution history. The similar chemical and mineral compositions of the obsidian and perlite glasses indicate their origin from the same silicic melt. The crystals of the minerals observed in both rocks are almost parallel to the lava flow, which indicates their formation before the final lava solidification. The perlite is extremely brittle due to a large number of microscopic cracks, which enables disclosure

of the obsidian glassy balls (marekanite) when the rock breaks apart.

The electron microprobe study has shown certain yet not fundamental differences in the compositions of the obsidian and perlite glasses. These are mainly caused by hydration of the silicic melt. The differences in content of alkali elements can also be accounted for by the perlite hydration. In comparison with the obsidian, the perlite glass exhibits both higher degree of hydration and higher variability in the contents of alkalis. The glass of both the perlite and the obsidian balls is homogeneous except for a thin outer shell, which indicates the surface hydration of the obsidian. We assume that this hydration took place already in the solid state.

Acknowledgements. We are grateful to Pasquale Acquafredda and an anonymous reviewer and also the Editor-in-Chief for reviews and suggested improvements. R. Skála is thanked for editorial handling. This research has been financed by the Ministry of the Environment of the Czech Republic in the framework of international cooperation of the Czech Republic and Nicaragua.

References

- DENTON JS, TUFFEN H, GILBERT JS, ODLING N (2009) The hydration and alteration of perlite and rhyolite. *J Geol Soc, London* 166: 895–904
- FRIEDMAN I, SMITH RL (1958) The deuterium content of water in some volcanic glasses. *Geochim Cosmochim Acta* 15: 218–228
- FRIEDMAN I, SMITH RL, LONG WD (1966) Hydration of natural glass and formation of perlite. *Geol Soc America Bull* 77: 323–328
- HRADECKÝ P, MLČOCH B, MRÁZOVÁ Š, RAPPRICH V, HAVLÍČEK P, NOVÁK Z, OPLETAL M, ŠEVČÍK J, VOREL T (2002) Geological study of the natural hazards in the area of Matagalpa, central Nicaragua. *Czech Geological Survey Prague, INETER Managua*, pp 1–110 (in Czech)
- JOHANNSEN A (1932) *A Descriptive Petrography of the Igneous Rocks*. Chicago University Press, Chicago, Illinois, Vol. 2: pp 1–428
- JUDD JW (1886) On marekanite and its allies. *Geol Mag* 3: 241–248
- LE BAS MJ, LE MAITRE RW, STRECKEISEN A, ZANETTIN B (1986) A chemical classification of volcanic rocks on the total alkali–silica diagram. *J Petrol* 27: 745–750
- LJUNGGREN P (1960) A formation of marekanite at El Fiscal, Guatemala. *Geol Mag* 97: 49–53
- MARSHALL RR (1961) Devitrification of natural glass. *Geol Soc America Bull* 77: 1493–1520
- NOH JH, BOLES JR (1989) Diagenetic alteration of perlite in the Guryongpo area, Republic of Korea. *Clay Clay Miner* 37: 47–58
- PECCERILLO A, TAYLOR SR (1976) Geochemistry of Eocene calc-alkaline volcanic rocks from the Kastamonu area, northern Turkey. *Contrib Mineral Petrol* 68: 61–81
- POUCHOU JL, PICOIR F (1985) “PAP” (ρ - ρ -Z) procedure for improved quantitative microanalysis. In: ARMSTRONG JT (ed) *Microbeam Analysis*. San Francisco Press, pp 104–106